Strong-Field Excitation of Helium: Bound State Distribution and Spin Effects

H. Zimmermann,[1,*] J. Buller,[1,†] S. Eilzer,[1] and U. Eichmann[1,2,‡]
[1]*Max-Born-Institute, Max-Born-Straße 2a, 12489 Berlin, Germany*
[2]*Institut für Optik und Atomare Physik, Technische Universität Berlin, 10623 Berlin, Germany*
(Received 9 September 2014; revised manuscript received 4 December 2014; published 24 March 2015)

Using field ionization combined with the direct detection of excited neutral atoms we measured the distribution of principal quantum number n of excited He Rydberg states after strong-field excitation at laser intensities well in the tunneling regime. Our results confirm theoretical predictions from semiclassical and quantum mechanical calculations and simultaneously underpin the validity of the semiclassical frustrated tunneling ionization model. Moreover, since our experimental detection scheme is spin sensitive in the case of He atoms, we show that strong-field excitation leads to strong population of triplet states. The origin of it lies in the fact that high angular momentum states are accessible in strong-field excitation. Thus, singlet-triplet transitions become possible due to the increased importance of spin-orbit interaction rather than due to direct laser induced spin-flip processes.

DOI: 10.1103/PhysRevLett.114.123003 PACS numbers: 32.80.Rm, 42.50.Hz

Understanding essential phenomena in atomic strong-field physics relies a great deal on intriguing pictures such as those linked to the simple man's or rescattering model [1–4]. These models are based on the dynamics of a quasifree electron driven by the laser field that can be considered a classical electric field. They are well supported by theory within the framework of the strong-field approximation or Keldysh-Faisal-Reiss approach, which retains only the ground state of the atom and neglects the Coulomb field after the electron has been liberated from the atom [5–8]. Over the last few years, however, experimental features have been unraveled, where the Coulomb field plays an increasing role in the understanding of experiments. Particularly worth mentioning are the observations of Coulomb focusing [9–12], strong-field holography [13] and low energy structure (LES) in strong-field ionization [14–16]. A striking case in this context is the strong-field excitation [9,17–21], where, in contrast to strong-field ionization, the inclusion of the Coulomb interaction is indispensable and must be treated on equal footing with the laser field. The frustrated tunneling ionization (FTI) process, a recently established important exit channel of an extended version of the simple man's or rescattering model, in which the Coulomb field is considered explicitly, predicts the n distribution of excited states in the tunneling regime of strong-field ionization [20,22]. While these predictions are backed up by quantum mechanical calculations [20,23], the experimental confirmation, which would put the idea of describing excitation within the tunneling model on solid ground, is still pending.

This Letter serves two purposes. The first purpose is to report on the experimental investigation of the n distribution of Rydberg states after strong-field excitation of He with intensities well in the tunneling regime. To measure an n distribution covering a large range of n including low n states around $n = 8$, as expected from theory, we apply a modified version of the field ionization method [24]. Rather than detecting ions or electrons produced by the field ionization process we measure the surviving excited state population [20,21,25]. The second purpose is to elucidate the role of the spin in strong-field excitation.

The setup of our experiment is outlined in Fig. 1. In an ultrahigh vacuum chamber with a background pressure below 10^{-8} mbar a highly collimated effusive beam of He atoms from a nozzle is passed through a pair of copper field plates with diameters of 15 mm and a separation of the plates of (1.00 ± 0.04) mm. A linearly polarized laser beam with a pulse duration of 45 fs full width at half maximum (FWHM) and a center wavelength of 800 nm intersects the atomic beam midway between the field plates. The laser is focused by means of a lens with 250 mm focal length. The resulting focal beam waist of

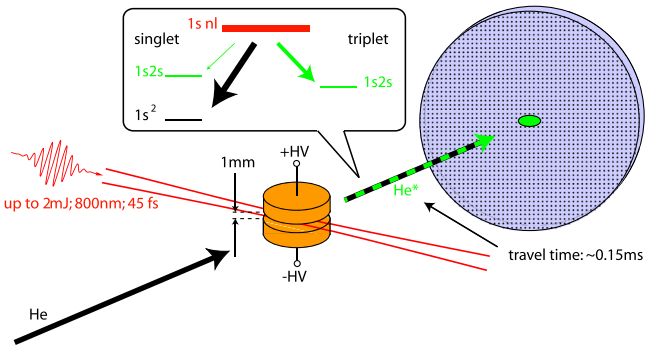

FIG. 1 (color online). Sketch of the experimental setup, which is explained in the text. The panel illustrates the radiative decay of the initial laser excited distribution (red) into the detectable metastable states (green) and the nondetectable ground state (black). The thickness of the arrows roughly depicts the probability of population.

$w_0 = (25 \pm 2)$ μm finally enables us to deliver peak laser intensities around a few times 10^{15} W/cm^2 to excite He atoms [20]. The atomic beam is directed towards a position sensitive microchannel plate detector. Excited and ground state atoms reach the detector after a mean time of flight of about 150 μs, while ions and electrons are removed from the beam. However, only atoms that are still in an excited state can be detected [26]. State-selective field ionization is achieved by applying two synchronized high-voltage pulses of opposite polarity, which are supplied by fast transistor switches, to the upper and lower field plate. As a result, we are able to provide electric field pulses reaching 65% of the maximum electric field after ≈150 ns and reaching their full amplitude of up to 250 kV/cm after ≈600 ns, with noise and ringing associated with the fast switching minimized by the balanced setup. With this field strength we are able to field ionize Rydberg atoms with principal quantum numbers as low as $n \approx 6$ according to the saddle point model of field ionization [24].

We record the He* yield as a function of the field strength of the field pulse that is applied shortly (<50 ns) after the strong-field laser excitation, see Fig. 2, curves (a). Since the intensities are close to the saturation intensity, the total yield does not change much. Applying instead a static electric field of the same strength the recorded He* yield is strikingly different, compare green triangles with black open squares in Fig. 2. Consequently, before we derive n distributions from the data, we will shed light on the peculiar experimental observations in static electric fields,

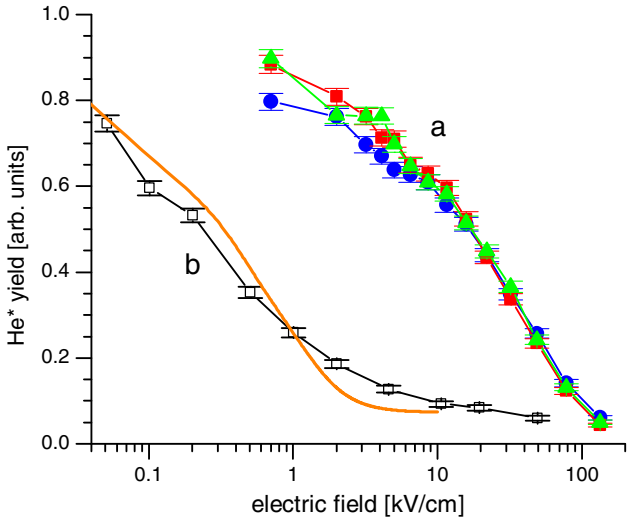

FIG. 2 (color online). Yield of excited He* atoms as a function of the field strength (a) of an electric field pulse applied shortly after the laser pulse for laser intensities 1.8×10^{15} W/cm^2 (blue dots), 2.2×10^{15} W/cm^2 (green triangles), and 2.9×10^{15} W/cm^2 (red squares), and (b) of a static electric field at a laser intensity of 2.2×10^{15} W/cm^2 (black open squares). The full orange curve in (b) is the result of a calculation, described in the Supplemental Material [27].

which allows us to extract valuable information about the role of the spin.

First, we recall the excitation process. Excitation of He ground state atoms ($1s^2\ ^1S$) with linearly polarized light results in final excited states $1snl$ with magnetic quantum number $m_l = 0$, if one assumes the validity of the dipole approximation and LS coupling, i.e., $\Delta m_l = 0$ and $\Delta S = 0$ transitions only. This goes along with practically forbidden intercombination transitions between singlet and triplet states. However, they are only forbidden as long as low angular momentum states with $l < 3$ are involved. For higher l states the LS coupling scheme breaks down and with respect to the LS coupled basis the two spin components are nearly equally mixed [31]. As a consequence, one might expect excitation of triplet states with equal probability to singlet state excitation for states with $l > 2$. More precisely, we can state that the strong laser field excites a spin wave packet, which is composed of both singlet and triplet admixtures, via its singlet component. Additionally, one might also conceive that the dipole approximation is no longer strictly valid and appreciable excitation of triplet states comes about through the strong magnetic field of the laser pulse which drives the spin-flip transition [32]. Although this process could be fortified by the motion of the laser-driven electron in the vicinity of the Coulomb field that causes additional spin-orbit interaction [33], we do not expect this effect to be present at our laser intensities.

Next, we consider the fluorescence decay of the initially excited states. Using known decay rates [34] we calculate that during the long time of flight of the atoms towards the detector nearly all states with $n < 25$ and $l < 10$ decay either into the ground state, which we cannot detect, or into the metastable states $1s2s\ ^{1,3}S$, which we detect. The probability to find an initially excited atom finally in an excited state (metastable state) at the detector, which we call detection probability in the following, is very different for pure singlet and triplet states.

Neglecting the intercombination transitions between singlet and triplet states for the time being and using again the decay rates [34] we can furthermore calculate that an initially excited nl singlet state would decay only by $\lesssim$1% into the detectable $1s2s\ ^1S$ metastable state. On the other hand, an initially excited triplet state would decay exclusively into the $1s2s\ ^3S$ triplet metastable state, which means 100% detection probability. If we take intercombination transitions into account [34], excited singlet states with orbital angular momentum $l < 2$ remain in the singlet system and thus, still have a low detection probability of $\lesssim$1%. However, all excited states with higher l quantum numbers decay through a cascade towards lower states and are finally bound to pass through the bottleneck of nf to $n'd$ transitions, where intercombination transitions occur for all n [34]. For higher $l > 2$ states they boost the detection probability for singlet states up to 30%–40% and reduce the

100% detection probability for triplet states by 30%. Important to note is that the detection probability of an initially excited He atom, despite its radiative decay, is to a large extent independent of its initial n and l quantum numbers, as long as $l > 2$.

Taking the above arguments it is reasonable to assume that the observed strong decrease of the He* yield already at low static field strengths is caused by suppression of the singlet-triplet mixing and not due to field ionization. Suppressed singlet-triplet mixing in electric fields, which finds its origin in the different polarizabilities of the singlet and triplet states, has been observed before in experiments, where He atoms are excited by proton impact [35]. We have confirmed this decoupling in a simplified rate equation model as detailed in the Supplemental Material [27]. We obtain the curve shown in 2(b), which favorably compares with the data. We note that we have observed directly the strong-field population of triplet states in a separate experiment using a Stern-Gerlach type setup [36].

We can go a step further and corroborate experimentally, that triplet states are already formed in the excitation process, and not only produced in a secondary process during the decay. In Fig. 3 we show measurements where we recorded at a fixed laser intensity the He* yield as a function of the field strength. The parameters we varied are the timing and the duration of the applied field pulse. The blue diamonds represent measurements, where the field pulse was applied 1 μs before the laser pulse and lasted after the laser pulse for (14, 1, and 0.06) μs, indicated by (a)–(c), respectively. Thereby, a field pulse duration of 14 μs corresponds roughly to the average travel time of the atoms between the field plates and thus appears for the atoms as a quasistatic field. Indeed, the blue diamonds in curve (a) are almost identical to the measurement with a static field applied, black open squares. Singlet-triplet mixing is obviously suppressed both in the excitation as well as in the decay. Thus, only the singlet states are involved, which have a low detection probability. Thus we can practically exclude a direct spin-flip transition from $S = 0$ to $S = 1$ during the laser pulse. When we decrease the duration of the field pulse, (b) and (c), the He* yield increases. It increases the most at higher electric field strengths, where the singlet-triplet decoupling is strongest, less at lower field strengths, where only partial decoupling is retained. This indicates that, while singlet-triplet mixing is suppressed during the laser pulse, the triplet states must be populated in the subsequent fluorescence decay. For the shortest pulse duration (c), the signal has increased by a factor of 10 for the highest field. As expected from the bottleneck transitions described before we detect roughly one third of the signal compared with the case, where no field is present during the laser excitation. Finally, when we inspect the two curves, where the field pulse was applied 14 ns after the laser pulse (d), we find that the different field pulse durations (1 and 20) μs, black dots and red dots, respectively, do not make a difference in the yield, as expected. This is a result from the fact that singlet and triplet excitation formation is initiated by the laser pulse in the first place, and the bottleneck transitions do not alter the detection any more.

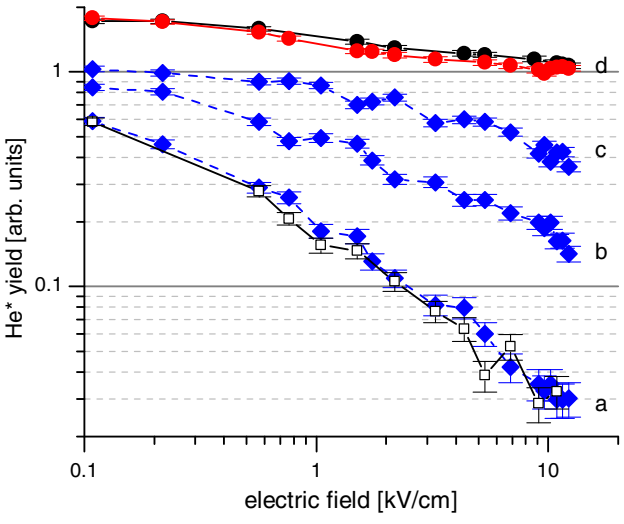

FIG. 3 (color online). He* yield as a function of the electric field strength at a laser intensity of 2.3×10^{15} W/cm^2. See text for more information.

We now turn towards extracting n distributions from the experimental data shown in Fig. 2(a). We convert the field strength scale into an n scale by exploiting the classical saddle point formula of the field ionization model $F = 1/16n^4$ [24]. This is valid as long as the field ionization proceeds adiabatically, which we assume to be fulfilled for our timing conditions of the field pulse and for the $m_l = 0$ subspace of excited states. Since our field ionization measurements are cumulative by nature, we obtain the n distribution by taking the derivative of the measured signal, as shown in Fig. 4.

Within the given error bars the experimental data are almost independent of the laser intensity and show a maximum in the population around $n = 9$, followed by a strong decrease of population for higher n, with some structure around $n = 15$. This might hint on resonant enhancement in the excitation process. However, due to the relatively large error bars in this region, the statistical significance of the data is limited. For comparison with theory we use the results from calculations using the semiclassical FTI model [20,22] and from quantum mechanical (QM) calculations within the single-active electron (SAE) approach. The QM calculations rely on an improved model potential [37] compared to the results presented in [20]. The Schrödinger equation is integrated over the full laser pulse width [38]. Both calculations do not consider the spin. The results are displayed in Fig. 4 and show a remarkable agreement with the experimental data. The maximum of the distribution is satisfyingly confirmed

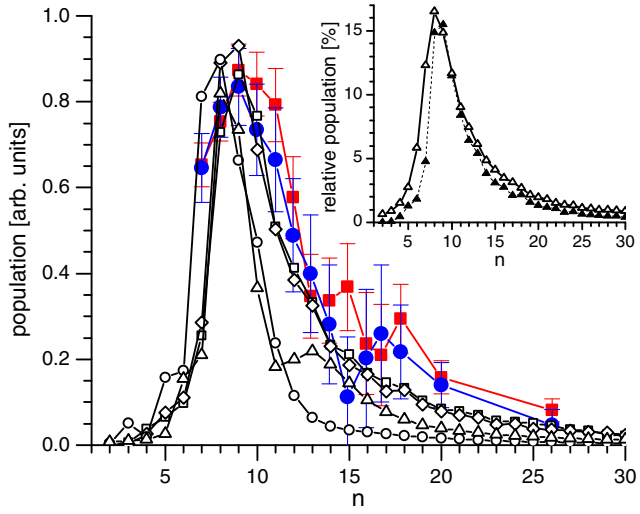

FIG. 4 (color online). Measured n distributions for a laser intensity 1.8×10^{15} W/cm^2 (blue dots) and 2.9×10^{15} W/cm^2 (red squares). Corrected calculated He* yield: classical FTI model at field strengths of 10^{15} W/cm^2 (open diamonds) and 1.4×10^{15} W/cm^2 (open squares) and quantum mechanical SAE calculations for laser intensities 1.8×10^{15} W/cm^2 (open circles) and 2.9×10^{15} W/cm^2 (open triangles). The inset shows for the FTI calculation (laser intensity 10^{15} W/cm^2) the difference between the distribution corrected for the state detection efficiency (open triangles) and the uncorrected one (filled triangles).

by both theories, whereby the predictions of the FTI model lie a little closer to the experimental data than the ones of the SAE calculations. The results of the classical calculations show only little intensity dependence in the range under study. It results only in a small change of the relative n population in the vicinity of the maximum. The overall yield of excited neutrals, however, varies in the range of 1%–2% of the ion yield. In order to stay within the tunneling picture the laser intensities used in the classical FTI calculations are restricted to the regime of "below barrier ionization." The laser intensity used in the QM calculations is not limited. The results confirm the weak intensity dependence even in the "above barrier regime," when inspecting the maximum of the distribution. The population of Rydberg states in higher n states, however, increases strongly relative to the maximum of the distribution with increasing laser intensity so that a sufficient population of higher Rydberg states is only achieved at the highest laser intensity.

So far we have neglected details of our specific detection process on the n distribution. In order to account for them we have weighted the theoretical n distributions, in which each n is a sum of the population of different l states, with the experimental state detection efficiency, as discussed above. This has been accomplished by solving rate equations for the fluorescence decay, where we have, beside using known fluorescence decay rates [34], additionally considered the influence of black body redistribution and the rise time of the field ionizing pulse. As can be inferred from the inset, corrections to the n distributions are small. Thus, we prefer to compare the experimental data with the uncorrected distributions.

The results can be discussed further in view of existing measurements of Rydberg state populations after strong-field excitation. In Ref. [19] strong-field excitation of Kr has been reported, where Rydberg states have been detected in the range $n = 14$ to 50 with almost equal probability of less than 1% of the single charged signal on total. The observation of a constant population is in fair agreement with our current results. On the other hand, photoionization of strong-field populated Xe atoms observe a large population of low lying states [18]. One should bear in mind, however, that the intensity used in those experiments is comparably low and well in the multiphoton regime, so that individual resonances might play an important role.

In conclusion, we have experimentally investigated the Rydberg state population after strong-field excitation of He atoms in the tunneling regime using a state selective field ionization method in combination with a direct detection technique of excited neutrals. We have confirmed the essential predictions of the frustrated tunneling ionization (FTI) model as well as of quantum mechanical calculations using a single-active electron approximation. With this we have established on firm grounds how excitation proceeds in the strong-field tunneling regime. Furthermore, due to the high angular momentum transferred to the atom we find that the spin-orbit effect becomes important, which, in turn, enables the efficient population of triplet states in the He atom. We infer that the laser pulse excites the singlet component of a spin wave packet where the singlet-triplet coupling is mediated by spin-orbit interaction of the field free atom.

We thank A. Saenz and E. Khosravi for providing the results of the quantum mechanical calculations and for fruitful discussions. We thank W. Becker for helpful comments on the manuscript.

*zimmerma@mbi-berlin.de
†Present address: Paul-Drude-Institute, Hausvogteiplatz 5-7, 10117 Berlin, Germany.
‡eichmann@mbi-berlin.de

[1] H. B. van Linden van den Heuvell and H. G. Muller, *in Multiphoton Processes*, edited by S. J. Smith and P. L. Knight (Cambridge University Press, Cambridge, 1988).
[2] T. F. Gallagher, Phys. Rev. Lett. **61**, 2304 (1988).
[3] K. C. Kulander, K. J. Schafer, and J. L. Krause, *Super-Intense Laser-Atom Physics* (Plenum, New York, 1993).
[4] P. B. Corkum, Phys. Rev. Lett. **71**, 1994 (1993).
[5] L. V. Keldysh, Sov. Phys. JETP **20**, 1307 (1965).
[6] F. H. M. Faisal, J. Phys. B **6**, L89 (1973).
[7] H. R. Reiss, Phys. Rev. A **22**, 1786 (1980).

[8] M. Lewenstein, P. Balcou, M. Y. Ivanov, A. L'Huillier, and P. B. Corkum, Phys. Rev. A **49**, 2117 (1994).
[9] G. L. Yudin and M. Y. Ivanov, Phys. Rev. A **63**, 033404 (2001).
[10] D. Comtois, D. Zeidler, H. Pepin, J. C. Kieffer, D. M. Villeneuve, and P. B. Corkum, J. Phys. B **38**, 1923 (2005).
[11] Y. Liu, D. Ye, J. Liu, A. Rudenko, S. Tschuch, M. Dürr, M. Siegel, U. Morgner, Q. Gong, R. Moshammer, and J. Ullrich, Phys. Rev. Lett. **104**, 173002 (2010).
[12] D. Shafir, H. Soifer, C. Vozzi, A. S. Johnson, A. Hartung, Z. Dube, D. M. Villeneuve, P. B. Corkum, N. Dudovich, and A. Staudte, Phys. Rev. Lett. **111**, 023005 (2013).
[13] Y. Huismans, A. Rouzée, A. Gijsbertsen, J. H. Jungmann, A. S. Smolkowska, P. S. W. M. Logman, F. Lépine, C. Cauchy, S. Zamith, T. Marchenko, J. M. Bakker, G. Berden, B. Redlich, A. F. G. van der Meer, H. G. Muller, W. Vermin, K. J. Schafer, M. Spanner, M. Y. Ivanov, O. Smirnova *et al.*, Science **331**, 61 (2011).
[14] C. I. Blaga, F. Catoire, P. Colosimo, G. G. Paulus, H. G. Muller, P. Agostini, and L. F. DiMauro, Nat. Phys. **5**, 335 (2009).
[15] W. Quan, Z. Lin, M. Wu, H. Kang, H. Liu, X. Liu, J. Chen, J. Liu, X. T. He, S. G. Chen, H. Xiong, L. Guo, H. Xu, Y. Fu, Y. Cheng, and Z. Z. Xu, Phys. Rev. Lett. **103**, 093001 (2009).
[16] T.-M. Yan, S. V. Popruzhenko, M. J. J. Vrakking, and D. Bauer, Phys. Rev. Lett. **105**, 253002 (2010).
[17] H. G. Muller, Phys. Rev. Lett. **83**, 3158 (1999).
[18] M. P. de Boer and H. G. Muller, Phys. Rev. Lett. **68**, 2747 (1992).
[19] R. R. Jones, D. W. Schumacher, and P. H. Bucksbaum, Phys. Rev. A **47**, R49 (1993).
[20] T. Nubbemeyer, K. Gorling, A. Saenz, U. Eichmann, and W. Sandner, Phys. Rev. Lett. **101**, 233001 (2008).
[21] U. Eichmann, T. Nubbemeyer, H. Rottke, and W. Sandner, Nature (London) **461**, 1261 (2009).
[22] S. Eilzer and U. Eichmann, J. Phys. B **47**, 204014 (2014).
[23] S. Chen, X. Gao, J. Li, A. Becker, and A. Jaroń Becker, Phys. Rev. A **86**, 013410 (2012).
[24] T. Gallagher, *Rydberg Atoms* (Cambridge University Press, Cambridge, 1994).
[25] U. Eichmann, A. Saenz, S. Eilzer, T. Nubbemeyer, and W. Sandner, Phys. Rev. Lett. **110**, 203002 (2013).
[26] W. Vassen, C. Cohen-Tannoudji, M. Leduc, D. Boiron, C. I. Westbrook, A. Truscott, K. Baldwin, G. Birkl, P. Cancio, and M. Trippenbach, Rev. Mod. Phys. **84**, 175 (2012).
[27] See Supplemental Material at http://link.aps.org/supplemental/10.1103/PhysRevLett.114.123003, which includes Refs. [28–30], for details on the singlet-triplet decoupling in electric fields.
[28] L. Windholz, T. J. Wasowicz, R. Drozdowski, and J. Kwela, J. Opt. Soc. Am. B **29**, 934 (2012).
[29] D. R. Cok and S. R. Lundeen, Phys. Rev. A **19**, 1830 (1979).
[30] D. R. Cok and S. R. Lundeen, Phys. Rev. A **24**, 3283 (1981).
[31] R. M. Parish and R. W. Mires, Phys. Rev. A **4**, 2145 (1971).
[32] M. W. Walser, D. J. Urbach, K. Z. Hatsagortsyan, S. X. Hu, and C. H. Keitel, Phys. Rev. A **65**, 043410 (2002).
[33] S. X. Hu and C. H. Keitel, Phys. Rev. Lett. **83**, 4709 (1999).
[34] G. W. F. Drake and D. C. Morton, Astrophys. J. Suppl. Ser. **170**, 251 (2007).
[35] A. Aynacioglu, G. Oppen, and R. Müller, Z. Phys. D **6**, 155 (1987).
[36] H. Zimmermann, S. Eilzer, and U. Eichmann (unpublished).
[37] A. Lühr, Y. V. Vanne, and A. Saenz, Phys. Rev. A **78**, 042510 (2008).
[38] E. Khosravi and A. Saenz (private communication).